

Inferred UV Fluence Focal-Spot Profiles from Soft X-Ray Pinhole Camera Measurements on OMEGA

W. Theobald, C. Sorce, W. R. Donaldson, R. Epstein, R. L. Keck, C. Kellogg, T. J. Kessler, J. Kwiatkowski, F. J. Marshall, S. Sampat, W. Seka, R. C. Shah, A. Shvydky, C. Stoeckl, L. J. Waxer, and S. P. Regan

Laboratory for Laser Energetics, University of Rochester

Laser-direct-drive inertial confinement fusion (LDD-ICF) implosions with cryogenically layered deuterium–tritium (DT) targets on OMEGA have produced hot-spot pressures >50 Gbar (Refs. 1 and 2), which is about half of the pressure required to achieve ignition conditions. Over the next several years the goal is to demonstrate an ignition-relevant hot-spot pressure of ~ 100 Gbar on OMEGA. The 100-Gbar Project includes improvements to the OMEGA Laser System, diagnostics, targets, and modeling, which will lead to a better understanding of the LDD-ICF physics. This requires a careful monitoring of each beam's intensity at full laser energy at the target plane, which is currently not possible, and is indirectly inferred from measurements outside the target chamber of the beam energy, the laser power, and the spot size. To characterize the focal spot of UV laser beams on target at full energy, a method was developed to image the soft x-ray emission from laser-irradiated Au planar foils. A pinhole camera with a back-thinned charge-coupled–device (CCD) detector and filtration with thin Be and Al foil filters provides images of the x-ray emission at photon energies <2 keV. This method requires a careful measurement of the relation between the applied UV fluence and the x-ray signal, which can be described by a power-law dependence. The measured exponent $\gamma \sim 2$ provides a dynamic range of ~ 30 for the inferred UV fluence. UV fluence profiles of selected beams were measured for 100-ps and 1-ns laser pulses and compared to directly measured profiles from an UV equivalent-target-plane (UVETP) diagnostic. The inferred spot size and super-Gaussian order from the x-ray technique agree within several percent with the values acquired by direct UV measurements. In an analogy to the UVETP technique, the method is called the x-ray target-plane (XTP) method, which is performed at full laser power inside the target chamber. UV fluence profiles were inferred for up to 11 beams equipped with SG5-850 distributed phase plates (DPP's) and were compared to directly measured UV profiles from the UVETP diagnostic for 4 of the 11 beams. Good agreement between the XTP and UVETP measurements was obtained, indicating that nonlinear optical effects from the transport in air and in the optics at the target chamber wall are likely negligible.

The experimental setup is depicted in Fig. 1(a). An OMEGA UV beam propagates from the left to the right side, passes through a distributed polarization rotator and reaches a fused-silica wedge—uncoated on the front and AR coated on the back—that picks up a 4% reflection of the full beam, which is then sent to the UVETP diagnostic. The main beam is then directed over a distance of about 18 m in air and passes through a DPP and a lens that focuses the beam onto a flat foil inside the target chamber. A similar DPP is placed in the UVETP diagnostic directly in front of an OMEGA focusing lens, mimicking the target/beam configuration. The beam is brought through focus in a vacuum tube, which is not shown in the simplified schematic; outside the tube, the expanding beam is picked up by another lens. The beam is down-collimated and attenuated, and a magnified image of the focus is produced on a CCD camera. The flat-foil target was a $20\text{-}\mu\text{m}$ -thick Si wafer with an area of $6 \times 6 \text{ mm}^2$ that was coated with a 500-nm layer of Au. The target normal was aligned along the axis of an opposing port with a ten-inch manipulator (TIM). Up to five beams were focused simultaneously onto the target such that the laser spots were well separated. A pinhole camera loaded into the TIM imaged the x-ray emission with a magnification of 5.16 onto a back-thinned CCD camera.

Figure 1(b) shows example data of the laser spot of Beam 56 from XTP and compares it to Fig. 1(c), the directly measured spot from UVETP. For a quantitative comparison of the fluence profiles, both images were fitted with an elliptical 2-D super-Gaussian function given by

$$F(x, y) = F_0 \exp \left\{ - \left[\left(\frac{x - x_0}{a} \right)^2 + \left(\frac{y - y_0}{b} \right)^2 \right]^{n_{SG}/2} \right\} + \text{back}, \quad (1)$$

where x_0, y_0 are the coordinates of the beam center, n_{SG} is the order of the super-Gaussian function, “back” is a constant background, and a and b are the minor and major axes of the ellipse, respectively. The fitting is performed over an area of $\sim 1.6 \times 1.6 \text{ mm}^2$ for both the UVETP and the XTP methods. The minimum signal included in the fit is $\sim 0.2\%$ of the peak signal for UVETP and $\sim 2\%$ of the peak signal for XTP. The spot radius is defined as the arithmetic mean of a and b :

$$R_{1/e} = \sqrt{a \cdot b}, \quad (2)$$

which describes the average radius where the fluence is at the $1/e$ value of the peak fluence F_0 . The two main parameters that are used to compare the fluence profiles are $R_{1/e}$ and n_{SG} . Figure 1(d) shows the result of the fitting process to the XTP image, while the residual (data minus fit) is shown in Fig. 1(e). The fit parameters were $R_{1/e} = 353.5 \pm 0.1 \text{ } \mu\text{m}$ and $n_{SG} = 4.86 \pm 0.01$, where the errors indicate the 95% confidence band from the fitting. The ellipticity was inferred with 0.8%, which means that the beam profile is close to circular. The fitting process of the UVETP data yielded $R_{1/e} = 358.4 \pm 0.0 \text{ } \mu\text{m}$, $n_{SG} = 5.03 \pm 0.00$, and an ellipticity of 1.4%. The fitting values from XTP are slightly lower than those from UVETP; however, this is not significant. The statistical errors for $R_{1/e}$ and n_{SG} were estimated by repeating the same measurement for the same beam over multiple shots and several campaigns. The errors for the XTP method are 1.0% and 3.4% for $R_{1/e}$ and n_{SG} , respectively, and 0.1% and 1.9% for the UVETP method, respectively. Systematic errors in the XTP method include magnification errors, calibration errors, and the limitation in dynamic range, which are estimated with $\sim 2.7\%$ and $\sim 4.5\%$ for $R_{1/e}$ and n_{SG} , respectively. With respect to the estimated error budget, the UV profiles from the XTP and UVETP diagnostics are in agreement.

The XTP data from 11 beams show some spread in spot size with Beam 52 having the largest spot ($R_{1/e} = 365.0 \text{ } \mu\text{m}$) and Beam 61 the smallest spot ($R_{1/e} = 345.9 \text{ } \mu\text{m}$). The difference in spot size between the largest and the smallest beams is $19 \text{ } \mu\text{m}$

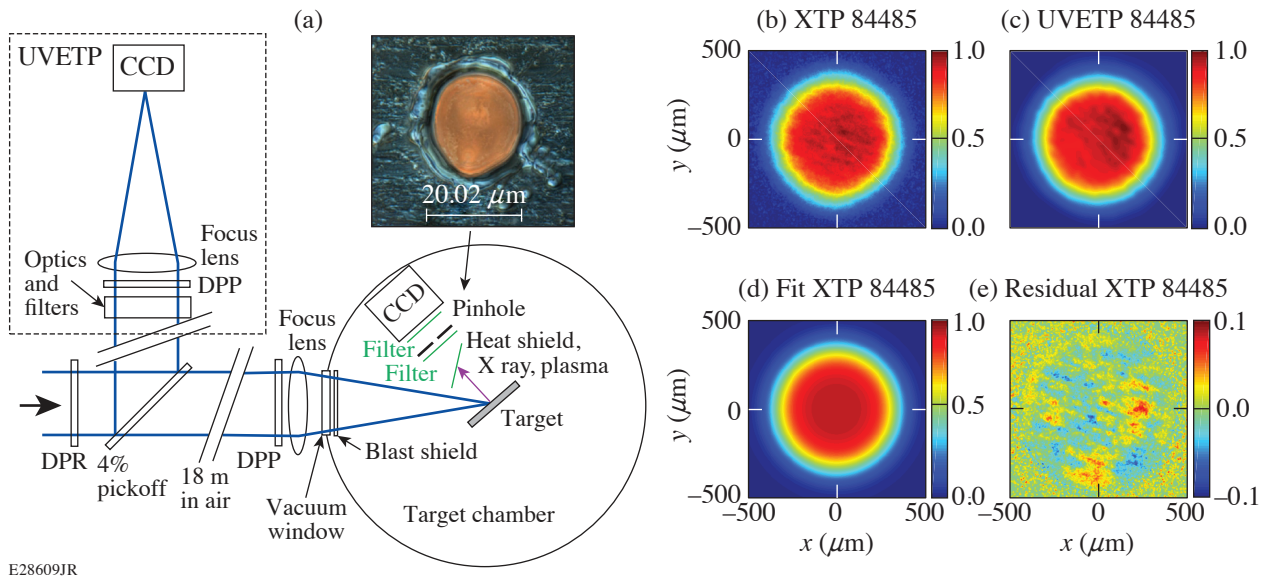


Figure 1

(a) Schematic of the experimental setup of the XTP and UVETP measurements including an optical image of a pinhole that measured the laser spots when using a 100-ps pulse. DPR: distributed polarization rotator. [(b)–(e)] UV laser-spot profiles from (b) XTP and (c) the UVETP diagnostic of Beam 56 for shot 84485. A 100-ps pulse was used. (d) The fitted 2-D super-Gaussian profile to the XTP image and (e) the residual of XTP (data minus fit).

($\sim 5\%$), which is larger than the measurement error; therefore, it is likely real. The peak fluence difference on target between Beams 52 and 61 is estimated with $\sim 11\%$. The average XTP values over the 11 beams resulted in $R_{1/e} = 356.6 \mu\text{m}$ and $n_{\text{SG}} = 4.92$. The average XTP values over those four beams that were covered by UVETP resulted in $R_{1/e} = 358.9 \mu\text{m}$ and $n_{\text{SG}} = 5.03$, which agree with the averaged UVETP data within the errors.

Figure 2 shows the beam-to-beam variation of the peak fluence normalized to the average value for (a) the 100-ps and (b) the 1-ns pulse measurements. The same energy was assumed on all beams. The red squares refer to the XTP diagnostic and the blue diamonds refer to the UVETP diagnostic. The yellow band indicates the acceptable rms variation (σ_{rms}) in peak fluence based on variation in beam shape, which is $\sigma_{\text{rms}} \approx 2\%$. The XTP data from the 11 beams indicate $\sigma_{\text{rms}} \approx 3\%$ for both the 100-ps and 1-ns pulse measurements, which is slightly larger than the acceptable variation. The UVETP data from the four beams result in $\sigma_{\text{rms}} \approx 1.5\%$, which is below the limit.

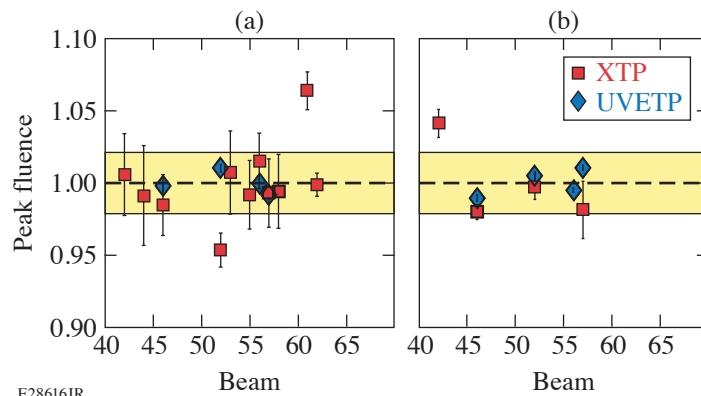


Figure 2
Beam-to-beam variation of the peak fluence normalized to the average value for (a) the 100-ps and (b) the 1-ns pulse measurements. The red squares refer to the XTP diagnostic and the blue diamonds refer to the UVETP diagnostic.

This material is based upon work supported by the Department of Energy National Nuclear Security Administration under Award Number DE-NA0003856, the University of Rochester, and the New York State Energy Research and Development Authority.

1. S. P. Regan *et al.*, Phys. Rev. Lett. **117**, 025001 (2016); **117**, 059903(E) (2016).
2. A. Bose *et al.*, Phys. Rev. E **94**, 011201(R) (2016).